Self-Immolative Nanoparticles Triggered by Hydrogen Peroxide and pH

Zhijian Wang, Jianbo Sun, Xinru Jia

Beijing National Laboratory for Molecular Sciences, Key Laboratory of Polymer Chemistry and Physics of the Ministry of Education, College of Chemistry and Molecular Engineering, Peking University, Beijing 100871, China
Correspondence to: X. Jia (E-mail: xrjia@pku.edu.cn)

Received 28 September 2013; accepted 31 March 2014; published online 00 Month 2014
DOI: 10.1002/pola.27203

ABSTRACT: The azomethine-based oligomers bearing boronate groups and imine moieties in the main chain were synthesized from a dialdehyde monomer and an aromatic (oligomer **4**) diamine or an aliphatic diamine (oligomer **5**). Based on the oligomers, the nanoparticles with hydrogen peroxide (H_2O_2) and pH dual-responsive properties were constructed and encapsulated nile red inside. The nanoparticles disassembled either by the trigger of H_2O_2 or by the attack of H^+, thus leading to the release of loaded species. Compared to oligomer **4**, oligomer **5** showed a faster degradation rate in the presence of H_2O_2, especially in a weak acidic environment. No significant cytotoxicity was observed as HeLa cells incubated in the nanoparticles with the concentration up to 200 μg/mL evidenced by cytotoxicity assay *in vitro*. Such a system capable of dual response of H_2O_2 and H^+ may have potential application as a carrier for drug delivery. © 2014 Wiley Periodicals, Inc. J. Polym. Sci., Part A: Polym. Chem. **2014**, *00*, 000–000

KEYWORDS: nanoparticles; oligomers; step-growth polymerization; stimuli-sensitive polymers

INTRODUCTION It is known that the excessive level of hydrogen peroxide (H_2O_2) (up to 1 mM)[1] will break the reactive oxygen species (ROS) balance and cause various human diseases including cancers, tissue damage, atherosclerosis, diabetes, and chronic hepatitis because of the occurrence of oxidation stress and damage to DNA.[2] However, H_2O_2, as a major source of ROS in living cells, is highlighted currently for its functions of regulating the intracellular signaling pathways and acting as a mediator in cell proliferation, differentiation, and migration.[3] In recent years, a number of drug carriers were developed with H_2O_2 as a trigger, such as H_2O_2-induced hydrophobic–hydrophilic transition,[4,5] oxidation of selenium-containing polymers,[6,7] cleavage of diselenide bond,[8] degradation of peroxalate ester bonds,[9] and disruption of boronate groups.[10–14] A typical example was reported by Fréchet and coworkers, who integrated the self-immolative structures into the dextran-based drug carrier.[15] In their case, the increased water-solubility of the polymer was ascribed to the disruption of hydrophilic–hydrophobic balance by a H_2O_2-induced oxidation reaction, leading to dissociation of the aggregates and liberation of the payloads. Recently, a self-immolative polymer responding to H_2O_2 has been reported.[16] Such main chain degradation polymer showed unique properties for the achievement of structure degradation and the release of loaded species.[17,18]

As reported, pHs in the intracellular compartments are different with near pH 5 in the late endosome and pH even lower in the lysosome.[19,20] Based on such behavior, many drug-delivery systems with pH sensitivity were reported to show the advantages of controlled and targeted drug release.[21–24] For example, Lahann and coworkers reported the synthesis of acetal-modified dextran that could be cleaved into hydrophilic dextran species in the presence of protons.[25] Besides, the polymers with tertiary amines or imidazole rings in the structure were also widely used in the design of carriers. Such polymers could transfer from hydrophobic to hydrophilic by the protonation, resulting in the release of payloads.[26]

Due to the sophisticated environments in the human body, it is imperative to create drug-delivery systems with multiple stimuli-responsive properties for precise control on both degradation kinetics and release of guest species. Up to now, many drug carriers with two triggers, such as reduction and pH, have been developed.[20,26,27] However, a drug-delivery system with the sensitivity of oxidation and pH is still rare, although some phagosomes are of oxidizability and acidic.[15] An example reported by Almutairi and coworkers described that the polythioether ketal that was cleaved in an acidic aqueous solution changed the hydrophobicity in the presence of H_2O_2.[5]

Herein, we report a new type of self-immolative nanoparticles from azomethine-based oligomers with the guest

Additional Supporting Information may be found in the online version of this article.

molecules inside. Our aim is to construct a dual responsive model system with H_2O_2 responsive moieties and pH sensitive groups in the main chain for exploring its potential application as a drug carrier. The nanoparticles disassembled either by breaking the boronate bonds with the trigger of H_2O_2, or by rupturing the C=N bonds at lower pHs.

EXPERIMENTAL

Measurements

^{1}H NMR spectra were recorded on 300 MHz (Varian Mercury) and 400 MHz (Bruker) spectrometers operated at room temperature with $CDCl_3$ or D_2O/acetone-d_6 as the solvents and tetramethylsilane (TMS) as the internal standard. The fluorescence spectra were recorded on a Hitachi F-4500 fluorescence spectrophotometer. Transmission electronic microscopy (TEM) measurement was operated by a JEM-100 CXII microscope with an acceleration voltage of 100 kV (Hitachi). The samples for TEM measurements were prepared as follows: a drop of the suspension was placed on a carbon-coated Formvar copper grid. After 2 min, the grid was tapped with filter paper to remove the aqueous solution on the surface and air-dried. Then, a drop of 1 wt % solution of uranyl acetate was added to the copper grid. The size of the nanoparticles was determined by dynamic light scattering (DLS) measurement at an angle of 90° (the ZetaPlus instrument, Brookhaven Instruments, NY). Gel permeation chromatography (GPC) measurement was performed on an Agilent 1200 series system, equipped with a VARIAN PolarGel-M column (300 × 7.5mm), an Iso Pump (G1310A), a UV detector at 254 nm, and a differential refractive index detector (RI). Except specially mentioned, the number average molecular weight (M_n) and the polydispersity (PDI) reported here were from the RI detector. *N*,*N*-Dimethylformamide (DMF) was used as the eluent at 50 °C with a flow rate of 1 mL/min. Narrowly distributed Poly(methyl methacrylate (MMA)) samples (molecular weight range of 690–1,944,000 g/mol, from Polymer Laboratories) were used as the calibration standard.

Both DLS and static light scattering (SLS) measurement of nanoparticles were performed on a Brookhaven goniometer (BI-200SM) equipped with a BI-TurboCorr digital correlator and a thermostatic bath with temperature accuracy of 0.01 °C. A vertically polarized solid-state laser operating at 532 nm was used as the light source (100 mW, CNI Changchun GXC-III, China). For a dilute solution, the root mean-square radius of gyration (R_g) can be obtained from SLS data on the basis of the following equation:

$$HC/R_{vv}(\theta)=(1/M_w)\left[1+(1/3)R_g^2q^2\right]+2A_2C$$

where $H=4\pi^2n^2(dn/dC)^2/(N_A\lambda^4)$, and $q=4\pi n/\lambda \sin(\theta/2)$, N_A, n, dn/dC, and λ are the Avogadro's number, the solvent refractive index, the specific refractive index increment, and the wavelength of light in a vacuum, respectively. In DLS, by using a Laplace inversion program, CONTIN, the normalized distribution function of the characteristic line width was obtained which could be further converted into the hydrodynamic radius R_h by using the Stokes–Einstein equation:

$$D=k_BT/6\pi\eta R_h$$

where D, k_B, T, η are the translational diffusive coefficient, the Boltzmann constant, the absolute temperature, and the viscosity of the solvent, respectively.

Materials

2,6-Dimethyl phenyl boronic acid (J&K Chemical Company), pinacol (Alfa Aesar), *N*-bromosuccinimide (NBS)(Alfa Aesar), and 4-hydroxy benzaldehyde (Alfa Aesar) were used as received. Azodiisobutyonitrile (AIBN) and *p*-phenylenediamine were recrystallized from methanol and ethanol, respectively. THF and chloroform was distilled following the standard procedures. Other solvents and reagents, unless stated specifically, were purchased from Beijing Chemical Reagent Co. and used as received.

Synthesis of Compound 1

About 10.0 g (67.0 mmol) 2,6-dimethyl phenylboronic acid and 9.50 g (80.4 mmol) pinacol were dissolved in 150 mL toluene in a 250-mL round bottom flask that was attached to a Dean-Stark apparatus. The mixture was heated to vigorous reflux and stirred for 6 h. Then, the solution was cooled to room temperature and toluene was evaporated *in vacuo*. The crude product was purified through a silica column using dichloromethane as the eluent. Compound **1** was obtained as a white solid. Yield: 92%.

Compound 1: ^{1}H NMR (400 MHz, $CDCl_3$, TMS, $T=298$ K): 7.12 (1 H, s), 6.93 (2 H, d, $J=7.6$ Hz), 2.39 (6 H, s), 1.38 (12 H, s). ^{13}C NMR (100 MHz, $CDCl_3$, TMS, $T=298$ K): 141.74, 129.14, 127.46, 126.40, 83.62, 24.95, 22.19. High Resolution-Electron Spray Ionization-Mass Spectroscopy (HR-ESI-MS): $C_{14}H_{22}BO_2$; Mass: calculated 233.17099, measured 233.17036.

Synthesis of Compound 2

About 3.51 g (15.1 mmol) compound **1**, 5.93 g (33.3 mmol) NBS, and 0.50 g (3.0 mmol) AIBN were dissolved in 25 mL tetrachloromethane in a Schlenk tube. After thoroughly deoxygenation, the tube was sealed and heated to 90 °C for 4 h. Then, the mixture was cooled to room temperature and filtrated. The filtrate was collected and purified through a silica column with petroleum ether/ethyl acetate (20/1) as the eluent. Compound **2** was obtained as a white solid. Yield: 95%.

Compound 2: ^{1}H NMR (400 MHz, $CDCl_3$, TMS, $T=298$ K): 7.33–7.20 (3 H, m), 4.89–4.75 (4 H, m), 1.52–1.39 (12 H, m). ^{13}C NMR (100 MHz, $CDCl_3$, TMS, $T=298$ K): 147.80, 144.08, 130.35, 129.83, 84.21, 33.90, 25.07. HR-ESI-MS: $C_{14}H_{23}BBr_2NO_2$; Mass: calculated 406.01836, measured: 408.01670.

Synthesis of Compound 3

About 1.00 g (2.56 mmol) compound **2** and 0.78 g (6.39 mmol) 4-hydroxybenzaldehyde were dissolved in 50 mL acetone followed by addition of 4 Å molecular sieves. Then,

3.54 g (2.56 mmol) anhydrous potassium carbonate was added into the mixture, stirred, and heated. After 8 h, the mixture was cooled to room temperature and filtrated. The filtrate was collected and evaporated *in vacuo*. The crude product was purified via a silica column with dichloromethane as the eluent. Compound 3 was obtained as a white solid. Yield: 41%.

Compound 3: ^{1}H NMR (400 MHz, $CDCl_3$, TMS, $T = 298$ K): 9.89 (1 H, s), 7.84 (2 H, d, J = 8.7 Hz), 7.08 (2 H, d, J = 8.7 Hz), 5.34 (2 H, s), 1.16 (6 H, s). ^{13}C NMR (100 MHz, $CDCl_3$, TMS, $T = 298$ K): 190.76, 163.85, 141.59, 131.95, 130.29, 130.02, 128.66, 115.03, 83.93, 70.49, 24.93. HR-ESI-MS: $C_{28}H_{30}BO_6$; Mass: calculated 473.21348, measured 473.21267.

Synthesis of Oligomer 4

About 94.4 mg (0.20 mmol) compound **3** and 21.7 mg (0.20 mmol) *p*-phenylenediamine were dissolved in 2 mL anhydrous chloroform in a Schlenk tube. After deoxygenation, the tube was sealed and heated to 90 °C for 24 h. After the solution was cooled to room temperature, the solvent was evaporated and a yellow solid was obtained. ^{1}H NMR (400 MHz, $CDCl_3$, TMS, $T = 298$ K): 9.90–9.87, 8.52–8.35, 7.92–7.76, 7.51–7.38, 7.17–6.98, 6.77–6.65, 5.39–5.23, 1.12–1.10.

Synthesis of Oligomer 5

About 198.2 mg (0.42 mmol) compound **3** and 24.0 mg (0.40 mmol) ethylene diamine were dissolved in 2 mL anhydrous chloroform in a Schlenk tube. After deoxygenation, the tube was sealed and heated to 90 °C for 24 h. After the solution was cooled to room temperature, the solvent was evaporated and a yellow solid was obtained. ^{1}H NMR (400 MHz, $CDCl_3$, TMS, $T = 298$ K): 9.90–9.87, 8.41–8.00, 7.72–7.56, 7.56–7.49, 7.49–7.32, 7.11–6.76, 5.39–5.05, 4.04–3.75, 1.34–0.87.

Preparation of the Nanoparticles

The nanoparticles were prepared by using a common emulsion method. About 1.56 mg oligomer **4** and 0.15 mg nile red was dissolved in 1 mL dichloromethane. The resulting red solution was added to a 0.1 M $NaHCO_3$ solution containing 1% Polyvinyl alcohol (PVA). The mixture was oscillated under ultrasound for 2 min and then the emulsion was stirred at room temperature. The suspension was purified by dialysis using a dialysis membrane ($M_w = 5000$) to remove PVA, then filtered using a 0.45-μm PES filter (Millipore) and followed by a 0.22-μm PES filter (Millipore). The size of nanoparticles was measured by particle sizing instrument and TEM.

H_2O_2-Triggered Degradation of the Oligomers

The degradation of oligomer **4** was measured by ^{1}H NMR measurement. The solution of 1 mg oligomer **4** in 200 μL acetone-d_6 was added into 300 μL 0.1 M $NaHCO_3$ solution in D_2O. The ^{1}H NMR spectrum of mixture was recorded via scanning in the 300 MHz NMR spectrometer for 12 h. Then, 0.5 μL 30% H_2O_2 was added into the NMR tube. After being incubated at room temperature for 24 h, the ^{1}H NMR spectrum was recorded again.

The degradation of oligomer **5** was conducted in the mixed solution of $CDCl_3$ and 0.1 M $NaHCO_3$. The solution containing 1 mg oligomer **5** in 500 μL $CDCl_3$ was added into 200 μL 0.1 M $NaHCO_3$ solution. The ^{1}H NMR spectrum of mixture was recorded via scanning in the 300 MHz NMR spectrometer for 12 h. Then, 0.5 μL 30% H_2O_2 was added into the system. After being incubated at room temperature for 24 h, the ^{1}H NMR spectrum was recorded again. The spectra were just of $CDCl_3$ phase.

The Release of Nile Red from Nanoparticles

The release of nile red was measured by the F4500 fluorescence spectrometer. The excitation and emission slit width of the fluorometer were set at 10 and 10 nm, respectively. The excitation wavelength was set up at 550 nm, and the emission spectra were recorded from 570 nm to 700 nm at a scanning rate of 60 nm/min. For the measurement, 30% H_2O_2 solution was added into the nanoparticle suspension for affording the resulting solution in the presence of H_2O_2 at different concentrations. HCl solution was added for adjusting a weak acidic environment. The fluorescence spectra were recorded at different time point. The excitation intensity value at 610 nm was used to record the release of nile red from the nanoparticles.

Cell Culture

HeLa cells were routinely grown in Dulbecco's Modified Eagle's Medium (DMEM) medium supplemented by 10% heated-inactivated fetal-bovine serum (FBS), 100 U/mL penicillin, and 100 μg/mL streptomycin. Cells were maintained at 37 °C with 5% CO_2.

In Vitro Cytotoxicity Assay

HeLa cells were seeded into 96-well culture plates at a density of 5×10^3 cells/well and grown for 24 h. Then, the nanoparticles prepared from the oligomers **4** and **5** were added into 96-well culture plates, respectively. The final concentrations of oligomers were controlled in the range of 0.1–200 μg/mL. After incubation for 48 h and staining the SRB assay, the cell viability was measured by a microplate reader at 549 nm. The following formula was used to calculate the cell survival:

$$\text{Survival}\,\% = (A_{540\text{nm}}\ \text{for the treated cells} / A_{540\text{nm}}\ \text{for the control cells}) \times 100\%$$

where the $A_{540\text{nm}}$ is the absorbance value. The cytotoxicity assay was repeated for three times.

RESULTS AND DISCUSSIONS

Generally, the imines from aromatic amines and aldehydes are more stable than those from aliphatic amines.[28] In order to understand the dependence of responsive property on the structure, oligomers **4** and **5** were designed with either aromatic or aliphatic Schiff base groups in the main chains. The oligomers were synthesized through a condensation polymerization from a dialdehyde monomer **3** containing a boronate group and an aromatic diamine (oligomer **4**) or an aliphatic (oligomer **5**) diamine. Scheme 1 depicts the

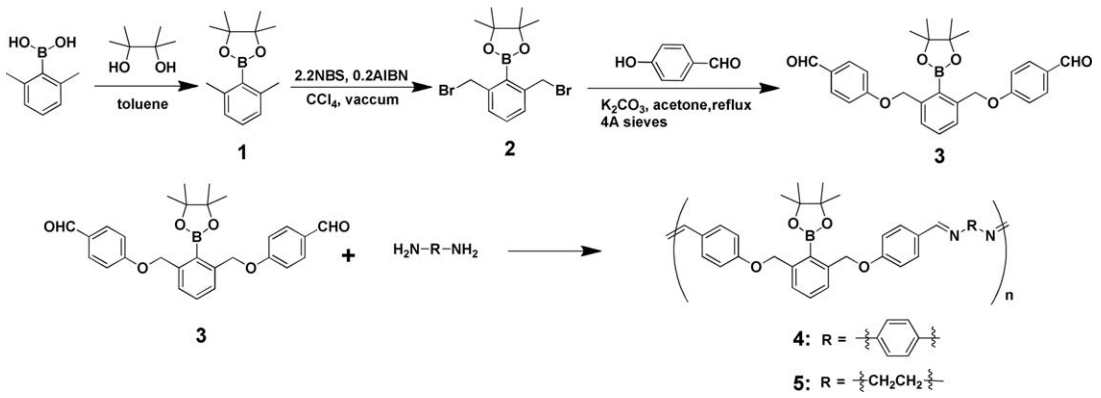

SCHEME 1 Synthesis and the structures of azomethine-based oligomers **4** and **5**.

structures of oligomers **4** and **5**. The detailed synthetic procedures and characterizations are described in the Experimental section.

Monomer **3** was prepared by the following reactions. Pinacol reacted with 2,6-dimethyl phenylboronic acid to generate boronic ester **1**. The bromination of methyl groups of **1** by NBS *in vacuo* afforded compound **2**. Monomer **3** was obtained via a typical etherification of 4-hydrophenyl aldehyde with benzyl bromide groups of **2**. Finally, the target oligomers **4** and **5** were simply synthesized by a well known necleophilic addition reaction between aldehyde groups of **3** and *p*-phenylenediamine or ethylene diamine, respectively.

The structures and molecular weight of **4** and **5** were characterized by ^{1}H NMR and GPC measurements (Supporting Information Figs. S1 and S2). It was found that the signal at 8.45 ppm related to the protons of azomethine appeared, indicating the formation of azomethine structure. From the integral ratio of aldehyde at 9.90–9.87 ppm and azomethine protons at 8.52 and 8.35 ppm, the repeating unit was calculated to be about 5 for both of the oligomers **4** and **5** in average, corresponding to the molecular weight of 2900 and 3500, respectively. The polydispersity of the obtained oligomers was also measured by GPC with the results of 2.28 for oligomer **4** and 2.07 for oligomer **5** (Supporting Information Fig. S2).

Scheme 2 depicts a proposed cleavage process of the azomethine-based oligomers. In the presence of H_2O_2, the boronates are oxidized and eliminated, which affords the hydroxyl groups in the oligomer structure. Then the oligomer chain undergoes an 1,4-quinone methide rearrangement, thus to cleave the ether bonds and generate the degradation products of 2,6-bis(hydroxymethyl) phenol, azomethine derivatives, and 4-hydroxy benzaldehyde. While in an acidic environment, N atom of Schiff base group is protonated, then by the attack of H_2O, the C=N bonds are ruptured to form the corresponding diamine and dialdehyde monomers.

The degradation of oligomers was confirmed by ^{1}H NMR measurement (Figure 1). Oligomer **4** was incubated for 24 h in the acetone-d_6/$NaHCO_3$/D_2O buffer solution containing 10 mM H_2O_2. As a result, the signals at 5.46 ppm corresponding to methylene protons of benzyl ether disappeared, indicating the breakage of benzyl ether structure. The proton signal of formyl groups shifted to high field at 9.5 ppm, and two doublet peaks near 7.78 and 6.75 ppm emerged obviously, confirming the formation of 4-hydrophenyl aldehyde (Supporting Information Fig. S3), one of the degradation products of oligomer **4**. However, the signals of the diimine were not observed because of its poor solubility in the mixed solvent.

Figure 2 shows the ^{1}H NMR spectra of oligomer **5**. It was incubated in a buffer of $CDCl_3$/$NaHCO_3$/D_2O containing 10 mM H_2O_2 or at pH 3 separately at room temperature for 24 h. We used a mixed solvent of $CDCl_3$/$NaHCO_3$/D_2O instead of acetone-d_6/$NaHCO_3$/D_2O buffer solution for ^{1}H NMR measurement because of the poor solubility of oligomer **5** in the later one. The spectra were just of the $CDCl_3$ phase. The

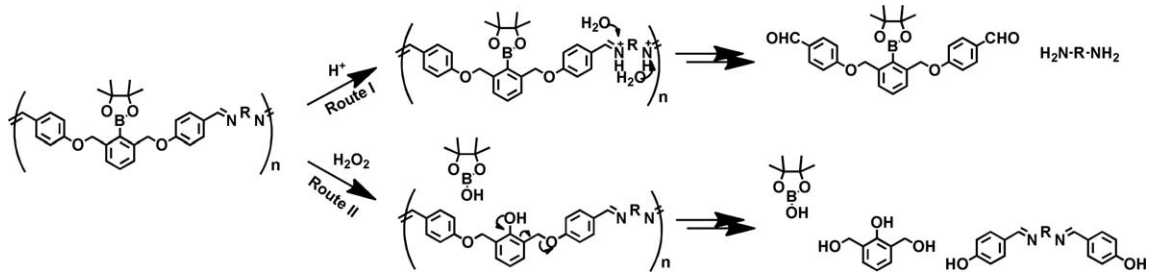

SCHEME 2 The proposed cleavage process of azomethine-based oligomers triggered by H_2O_2 and pH.

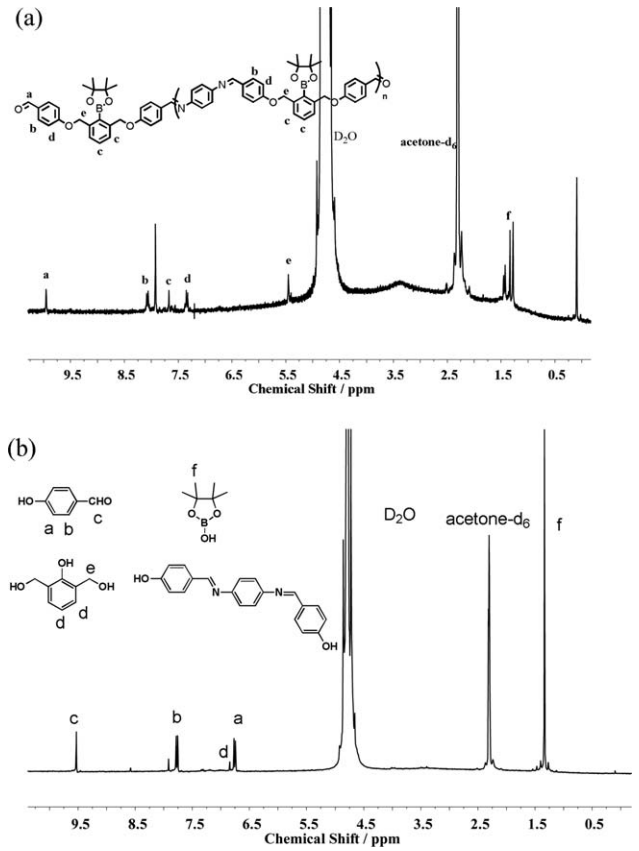

FIGURE 1 ^{1}H NMR spectra of (a) oligomer **4** in 0.1 M $NaHCO_3$ buffer (D_2O): acetone-d_6 (3:2); (b) oligomer **4** after incubated for 24 h in 0.1 M $NaHCO_3$ buffer containing 10 mM H_2O_2 (D_2O): acetone-d_6 (3:2).

peak at 3.91 ppm corresponding to the signal of ethyl diamine was not detected because the product transferred into the aqueous phase. Moreover, when the sample was incubated with 10 mM H_2O_2 for 24 h, the signals assigned to the methylene protons of 2,6-bis(hydroxymethyl) phenol appeared at 4.77 ppm, demonstrating the cleavage of ether bonds [Fig. 2(b)]. At pH 3.0, the signal at 9.98 ppm corresponding to the aldehyde protons increased obviously, and the signal at 8.21 ppm disappeared, approving the cleavage of C=N bonds [Fig. 2(c)].

The GPC traces also confirmed the degradation of oligomers by the oxidization of H_2O_2 or at an acidic environment (Supporting Information Fig. S4). As a result, the oligomers degraded into fragments with different length. The number-average molecular weight (M_n) of oligomers **4** and **5** decreased to 1900 and 1200 after being incubated in 100 mM H_2O_2 for 24 h. Moreover, the M_n of both oligomers **4** and **5** decreased to 600 at pH 3.

To investigate the release of guest species, we used a simple emulsion method[29–32] to prepare the nanoparticles with nile reds encapsulated inside for its good stability and as an excellent fluorescence probe in the presence of H_2O_2.[33–35]

The size of nanoparticles was measured by TEM and DLS at an angle of 90° by the ZetaPlus instrument. The size of particles from oligomer **5** was about 180 nm (TEM), and 230 nm (DLS) in average. While the nanoparticles from oligomer **4** were smaller with the size of about 50 nm (TEM) and 150 nm (DLS), which might be due to the stronger π–π interactions of aromatic groups in the structure of oligomer **4**.

The H_2O_2 responsive behaviour of nanoparticles was examined by the fluorescence spectroscopy using nile red as a probe whose emission intensity would decrease when transferred from hydrophobic environment into an aqueous medium. Figure 3 shows the plots of normalized fluorescent intensity of nile red vs. time when the nanoparticles were treated with H_2O_2 at different concentrations. It shows that the emission intensity remains constant without H_2O_2, but reduces over time upon treated with H_2O_2, indicating the disassembly of nanoparticles and the release of payloads into the aqueous solution. We noticed that the nanoparticles from oligomers **4** and **5** displayed different degradation rates, particularly by increasing the concentration of H_2O_2. At the concentration of 10 mM, the emission intensity of nanoparticles from oligomer **5** reduced to 60%, while for the nanoparticles from oligomer **4**, it was 85%. With increasing the concentration of H_2O_2 to 100 mM, the emission intensity of nanoparticles from oligomer **5** decreased rapidly to 40% within a short time (60% for the particles from oligomer **4** under the same condition), indicating the nanoparticles from oligomer **4** degraded slower. That might be because its dense structure gave difficulty for the attack of H_2O_2.

To understand the disassembly of nanoparticles, we observed the morphologies of nanoparticles before and after treating with H_2O_2 by TEM. The images are shown in Figure

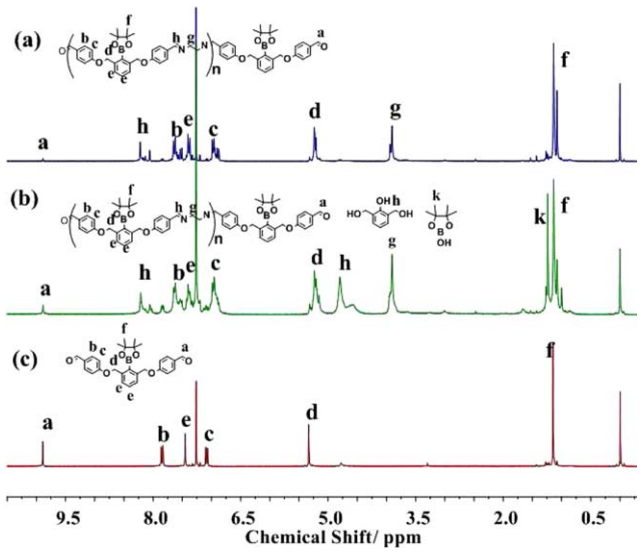

FIGURE 2 ^{1}H NMR spectra of oligomer **5** incubated in a mixed solvent of buffer (D_2O) containing 0.1 M $NaHCO_3$ and $CDCl_3$ (1:5) (a) without H_2O_2, (b) with 10 mM H_2O_2, and (c) at pH 3 for 24 h at room temperature. [Color figure can be viewed in the online issue, which is available at wileyonlinelibrary.com.]

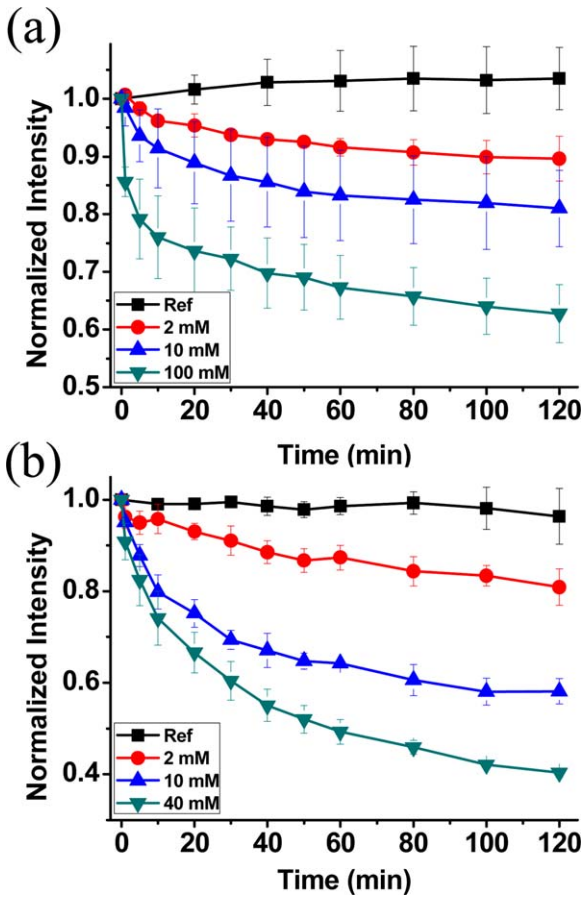

FIGURE 3 The plots of time vs. emission intensity (at 610 nm) of nile red encapsulated in nanoparticles treated with different concentrations of H_2O_2 (a) from oligomer **4** and (b) from oligomer **5**. [Color figure can be viewed in the online issue, which is available at wileyonlinelibrary.com.]

4 and Supporting Information Figure S5, respectively. The nanoparticles are sphere-like in original [Fig. 4(a)]. The loose particles with larger size [Fig. 4(b)] were observed when incubated the particles in a solution containing 100 mM H_2O_2 for 24 h, which evidences the disassembly process. Such phenomenon is in accordance with the report by Almutairi and coworkers who found that the polymeric particles expanded and ripped when exposed to H_2O_2.[16] Interestingly, we found that the nanoparticles from oligomer **5** (Fig. 4) showed a more serious ruptured morphology than that from

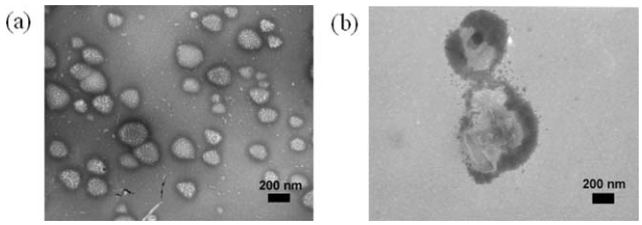

FIGURE 4 TEM images of nanoparticles prepared from **5** incubated (a) without H_2O_2 and (b) with 100 mM H_2O_2 for 24 h.

oligomer **4** (Supporting Information Fig. S5), suggesting the superior sensitivity of oligomer **5** to H_2O_2. The results were in agreement with the degradation kinetics measured by fluorescence spectroscopy. We also tried DLS measurement to observe how the size of nanoparticles from oligomer **4** and oligomer **5** changed according to the time of adding H_2O_2. However, $R_{h,app}$ did not show any significant change after the addition of H_2O_2 because the particle size distribution is too broad to give the useful information (Supporting Information Fig. S6).

Moreover, we noticed that the H_2O_2-triggered cleavage reaction was speeded up at a weak acidic environment. The fluorescent intensity was 60% in a buffer solution with 10 mM H_2O_2 at pH 8.5, it dropped to nearly 40% at pH 5.0, while it was 85% at pH 5.0 without H_2O_2. The results demonstrated that the enhanced degradation and release efficiency were achieved in a weak acidic medium and low concentration of H_2O_2. Such conditions are more close to the physiological environment.

However, the situation was different at pH 3.0. The intensity decreased to 40% either at pH 3.0 or at pH 3.0 with 10 mM H_2O_2 in the system, which might be due to the rupture of C=N groups dominating the degradation because of the strong protonation of imine groups at pH 3.0 as shown in Figure 5(a,b).

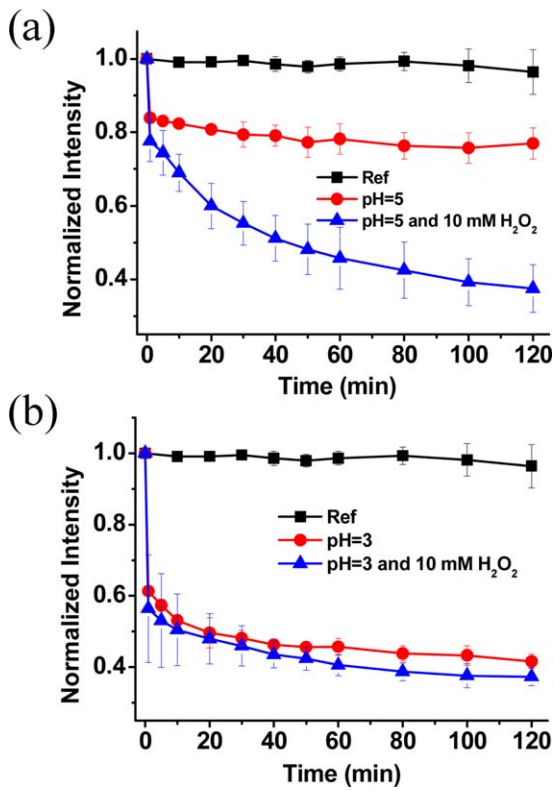

FIGURE 5 The plots of time vs. emission intensity of nile red (at 610 nm) encapsulated in nanoparticles (oligomer **5**) at (a) pH 5 and (b) pH 3. [Color figure can be viewed in the online issue, which is available at wileyonlinelibrary.com.]

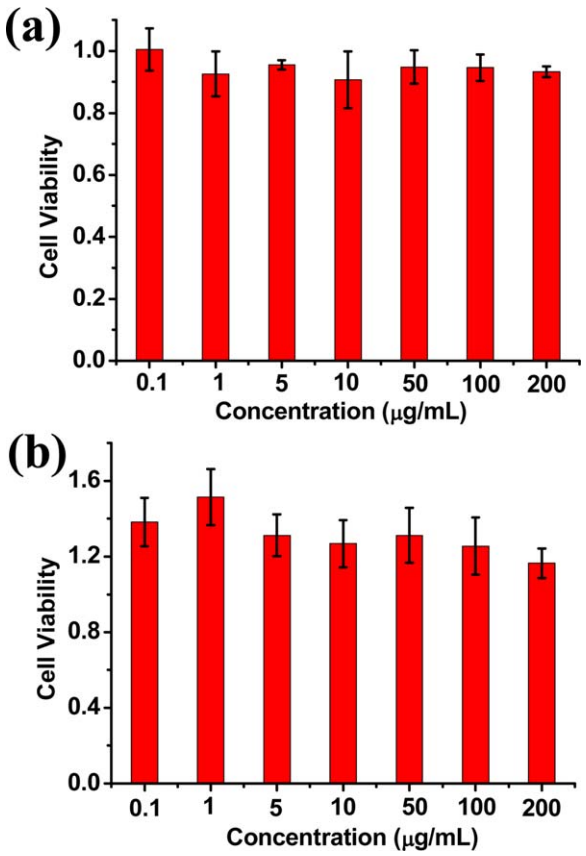

FIGURE 6 Cytotoxicity of nanoparticles prepared from (a) oligomer **4** and (b) oligomer **5** at different concentrations for HeLa cells. The cells were incubated with the nanoparticles for 48 h. [Color figure can be viewed in the online issue, which is available at wileyonlinelibrary.com.]

Both of the nanoparticles showed pH sensitivity for containing imine moieties in the backbone. Taking the nanoparticles from **5** as an example, it could be seen that the fluorescent intensity reduced with the pH values changing from 8.5 to 5.0 [Fig. 5(a)], and further decreased dramatically at pH 3.0 [Fig. 5(b)], which indicated that the release of nile red was accelerated at lower pH. That means the lower the pHs, the more cleavage of the C=N bonds.

We evaluated the cytotoxicity of nanoparticles prepared from the oligomers by SRB assay using HeLa cell line. HeLa cells were incubated in the nanoparticles with the concentrations ranging from 0.1 μg/mL to 200 μg/mL for 48 h. Figure 6 shows the cytotoxicity of nanoparticles at different concentrations to HeLa cells. No significant cytotoxicity was observed when the cells incubated in the nanoparticles either from oligomers **4** or oligomer **5** with the concentration up to 200 μg/mL.

CONCLUSIONS

In conclusion, we designed and synthesized a new kind of H_2O_2 and pH dual responsive self-immolative nanoparticles based on azomethine oligomers with boronates and imine groups in the main chain. The nanoparticles from oligomers **4** and **5** degraded with the trigger of H_2O_2 via a 1,4-quinone methide rearrangement. In addition, the nanoparticles could also break into monomers and release the loaded species under acidic condition. Compared to oligomer **4**, oligomer **5** showed a faster degradation rate in the presence of H_2O_2, especially in a weak acidic environment. Such a system capable of dual response of H_2O_2 and H^+ may have potential application as a carrier for drug delivery.

ACKNOWLEDGMENTS

This work is financially supported by the National Natural Science Foundation of China (21174005 and 21274004) to X.R.J. The authors thank Dehai Liang for the help in the characterization of nanoparticles.

REFERENCES AND NOTES

1 E. Schroder, P. Eaton, *Curr. Opin. Pharmacol.* **2008**, *8*, 153–159.

2 G. Waris, H. Ahsan, *J. Carcinog.* **2006**, *5*, 14–14.

3 S. G. Rhee, *Science* **2006**, *312*, 1882–1883.

4 M. K. Gupta, T. A. Meyer, C. E. Nelson, C. L. Duvall, *J. Control. Release* **2012**, *162*, 591–598.

5 E. A. Mahmoud, J. Sankaranarayanan, J. M. Morachis, G. Kim, A. Almutairi, *Bioconjugate Chem.* **2011**, *22*, 1416–1421.

6 N. Ma, Y. Li, H. Ren, H. Xu, Z. Li, X. Zhang, *Polym. Chem.* **2010**, *1*, 1609–1614.

7 P. Han, N. Ma, H. Ren, H. Xu, Z. Li, Z. Wang, X. Zhang, *Langmuir* **2010**, *26*, 14414–14418.

8 N. Ma, Y. Li, H. Xu, Z. Wang, X. Zhang, *J. Am. Chem. Soc.* **2010**, *132*, 442–443.

9 J. Kwon, J. Kim, S. Park, G. Khang, P. M. Kang, D. Lee, *Biomacromolecules* **2013**, *14*, 1618–1626.

10 H. G. Kuivila, A. G. Armour, *J. Am. Chem. Soc.* **1957**, *79*, 5659–5662.

11 D. Srikun, E. W. Miller, D. W. Dornaille, C. J. Chang, *J. Am. Chem. Soc.* **2008**, *130*, 4596–4597.

12 L. C. Lo, C. Y. Chu, *Chem. Commun.* **2003**, 2728–2729.

13 E. Sella, D. Shabat, *Chem. Commun.* **2008**, 5701–5703.

14 E. Sella, D. Shabat, *J. Am. Chem. Soc.* **2009**, *131*, 9934–9935.

15 K. E. Broaders, S. Grandhe, J. M. J. Frechet, *J. Am. Chem. Soc.* **2011**, *133*, 756–758.

16 C. de Gracia Lux, S. Joshi-Barr, N. Trung, E. Mahmoud, E. Schopf, N. Fomina, A. Almutairi, *J. Am. Chem. Soc.* **2012**, *134*, 15758–15764.

17 Y. Zhao, *Macromolecules* **2012**, *45*, 3647–3657.

18 D. Han, X. Tong, Y. Zhao, *Macromolecules* **2011**, *44*, 437–439.

19 C. C. Cain, D. M. Sipe, R. F. Murphy, *Proc. Natl. Acad. Sci. USA* **1989**, *86*, 544–548.

20 J. Chen, X. Qiu, J. Ouyang, J. Kong, W. Zhong, M. M. Q. Xing, *Biomacromolecules* **2011**, *12*, 3601–3611.

21 W. Gao, J. M. Chan, O. C. Farokhzad, *Mol. Pharmaceut.* **2010**, *7*, 1913–1920.

22 X. Q. Yang, J. J. Grailer, I. J. Rowland, A. Javadi, S. A. Hurley, V. Z. Matson, D. A. Steeber, S. Q. Gong, *ACS Nano* **2010**, *4*, 6805–6817.

23 X. L. Wu, J. H. Kim, H. Koo, S. M. Bae, H. Shin, M. S. Kim, B. H. Lee, R. W. Park, I. S. Kim, K. Choi, I. C. Kwon, K. Kim, D. S. Lee, *Bioconjugate Chem.* **2010**, *21*, 208–213.

24 C. H. Lee, S. H. Cheng, I. P. Huang, J. S. Souris, C. S. Yang, C. Y. Mou, L. W. Lo, *Angew. Chem. Int. Edit.* **2010**, *49*, 8214–8219.

25 T. H. Park, T. W. Eyster, J. M. Lumley, S. Hwang, K. J. Lee, A. Misra, S. Rahmani, J. Lahann, *Small* **2013**, *9*, 3051–3057.

26 S. Yu, C. He, J. Ding, Y. Cheng, W. Song, X. Zhuang, X. Chen, *Soft Matter* **2013**, *9*, 2637–2645.

27 C. Wei, J. Guo, C. Wang, *Macromol. Rapid Commun.* **2011**, *32*, 451–455.

28 R. Nguyen, L. Allouche, E. Buhler, N. Giuseppone, *Angew. Chem. Int. Edit.* **2009**, *48*, 1093–1096.

29 L. Mu, S. S. Feng, *Pharmaceut. Res.* **2003**, *20*, 1864–1872.

30 K. Y. Win, S. S. Feng, *Biomaterials* **2005**, *26*, 2713–2722.

31 S. Hariharan, V. Bhardwaj, I. Bala, J. Sitterberg, U. Bakowsky, M. Kumar, *Pharmaceut. Res.* **2006**, *23*, 184–195.

32 D. K. Sahana, G. Mittal, V. Bhardwaj, M. Kumar, *J. Pharmaceut. Sci.* **2008**, *97*, 1530–1542.

33 C. Park, K. S. Choi, Y. Song, H. J. Jeon, H. H. Song, J. Y. Chang, C. Kim, *Langmuir* **2006**, *22*, 3812–3817.

34 S. K. Pal, D. Sukul, D. Mandal, K. Bhattacharyya, *J. Phys. Chem. B* **2000**, *104*, 4529–4531.

35 D. L. Sackett, J. R. Knutson, J. Wolff, *J. Biol. Chem.* **1990**, *265*, 14899–14906.